

POLARIZATION DEPENDENCE ON HIGH-ORDER REFLECTION SPECTROSCOPY OF ARTIFICIAL OPAL PHOTONIC CRYSTAL

LE DAC TUYEN^{a,†} AND VU DINH LAM^b

^a*Department of Physics,
Hanoi University of Mining and Geology,
18 Pho Vien, Bac Tu Liem, Hanoi, Vietnam*

^b*Institute of Materials Science,
Vietnam Academy of Science and Technology,
18 Hoang Quoc Viet, Hanoi, Vietnam*

[†]*E-mail: ledactuyen@humg.edu.vn*

Received 31 July 2017

Accepted for publication 01 August 2018

Published 31 August 2018

Abstract. *We present polarization- and angle-resolved optical reflection of a fine artificial opal photonic crystal consisting of SiO₂ spheres into a face-centered-cubic lattice. The measurement shows the polarization dependence on high-order reflection (energy region $a/\lambda = 1.0 - 1.5$). It is shown that the reflection peaks are strongly dependent on s- and p-polarized light illuminating on the sample. The experiment results are analyzed and compared with photonic bands which are obtained according to prediction based on group theory.*

Keywords: opal photonic crystals, reflection, polarization, band structure.

Classification numbers: 42.25.Ja, 42.70.Qs.

I. INTRODUCTION

The interaction of light with photonic crystals (PhCs) exhibits unique features due to its subwavelength nature of the surface and the periodic variation of refractive index in the depth of the crystals [1–4]. The understanding of optical properties of opal PhCs in the high frequency region is great importance, because it leads to realistic applications. Many exotic optical phenomena offer working mechanisms for optical devices based on photonic band gap [2–4]. Moreover, their novel nontrivial properties can be used to advance in fundamental aspects of the interaction of light and condensed media [2, 3].

Artificial opal structures consisting of face-centered-cubic (fcc) lattices of dielectric spheres are the most commonly studied example of three-dimensional PhCs because they provide platform ideas to study various optical properties of new structures [1]. Their fabrication processes are usually based on self-assembly of colloidal spheres, which is a simple and cheap way towards large-scale structures. However, the result in imperfect crystals contains point defects, dislocations, and domains which affect the optical properties and limit the applicability of opals in optical circuitry [5, 6]. A lot of work has been published on the optical characterization of opal PhCs including both theory and experiment [5–18]. The early works approached the optical properties in the first-order stop band which is low energy region ($a/\lambda < 1$, a is the lattice spacing and λ is the wavelength of light) [7, 8]. In the high-order stop band ($a/\lambda > 1$, high energy region), the noise and the broadening induced by defects become even more detrimental. As a consequence, good quality samples are required for investigation of optical properties of opal structures in this region [6, 11]. The polarization dependence on optical properties relating to lattice disorder of opal PhCs was analyzed [15, 16]. However, most of the optical measurements have discussed polarization dependence effects of the first- and second-order stop band. The polarization dependence on the high-order stop band, which is more complex and not easy to observe, has not been reported yet.

In this work, we report angle-resolved optical spectroscopy and analyze polarization dependence on the high-order reflection. The reflection measurement is carried out along L-U (L-K) orientation of the first Brillouin zone (FBZ). It shows experimental evidence of polarization dependence on interaction of polarized light with the spatially periodic structure. The reflection peaks are compared with photonic band structure according to predicted symmetry which was assigned by arguments based on group theory.

II. EXPERIMENT

Colloidal silica nanospheres (SiO_2) are synthesized following a method developed by Stöber et al. via the hydrolysis and condensation of tetraethoxysilane (TEOS - $\text{Si}(\text{OC}_2\text{H}_5)_4$) in mixtures of alcohol ($\text{C}_2\text{H}_5\text{OH}$), water (H_2O), and aqueous ammonia (NH_4OH) [9, 19]. The artificial opal PhC is fabricated by thermal-assisted cell method whose experimental details have been reported in previous work [9]. The morphology of artificial opal films is determined by scanning electron microscopy (SEM). The diffraction pattern of the opal PhC is generated by a He-Cd Laser with the wavelength at 325 nm.

The angle-resolved reflection spectroscopy of the opal PhC is measured using an Ocean-optic fiber spectrometer. Fig. 1 illustrates the schematic of reflection measurement setup. A tungsten halogen lamp was used as a light source that can produce a broadband spectrum in the visible

region. The p- and s-polarization of the collimated light are controlled by using a prism polarizer to adjust electric field vector as parallel (\mathbf{E}_p , $\varphi = 0^\circ$) and perpendicular (\mathbf{E}_s , $\varphi = 90^\circ$) to the plane of incidence, respectively. The cross-section diameter of the light beam is 1 mm. The reflected light beam is collected by a lens and focused to a fiber bundle which is connected to a spectrometer. The sample can be rotated by a rotation stage with an angular step of 1° . We carried out s- and p-polarized reflection measurement with the incident angle θ varying from 0° to 20° along the L-U (L-K) orientation of the FBZ in Fig. 1(b).

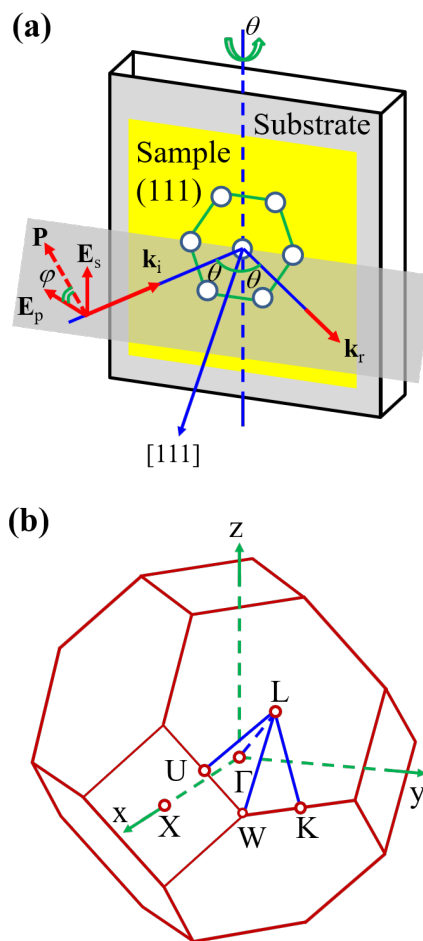


Fig. 1. (a) Schematic of experimental setup for polarization- and angle-resolved reflection spectroscopy on the opal structure: θ is incident angle, and φ is polarized orientation angle. (b) The first Brillouin zone of the fcc structure and symmetric points.

III. RESULTS AND DISCUSSION

The SEM image on the top surface of a SiO₂ opal PhC is shown in Fig. 2(a). Monodispersed SiO₂ nanospheres with a diameter of 424 nm were closely packed on the glass substrate. The thickness of the sample is about 20 μm. The Fourier transform of the SiO₂ opal is shown in Fig. 2(b), indicating hexagonal symmetry of SiO₂ nanospheres on uppermost (111) plane. Fig. 2(c) presents a photograph of the diffraction pattern corresponding to opal sample. Six diffraction spots are observed on a screen parallel to the sample when a laser beam of He-Cd Laser ($\lambda = 325$ nm, $a/\lambda = 1.846$) illuminated perpendicular onto the sample surface with a beam diameter of 1 mm. The orientation of the spots is unchanged when the illumination position on the sample is changed. The clear diffraction spots indicate the existence of fine crystalline structure in a long range [20]. It allows to identify the orientation of samples.

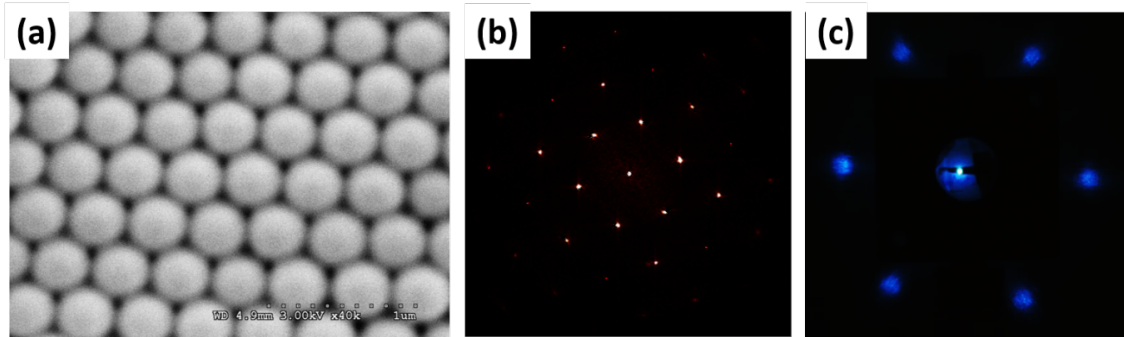


Fig. 2. (a) Top view SEM image of artificial opal PhC of SiO₂ nanospheres with the sphere diameter $D = 424$ nm. (b) Fourier transform and (c) Photograph of diffraction pattern of artificial opal PhC.

Reflection and transmission measurements are often used for studying optical properties of photonic crystals. The optical observation is explained by means of multiple diffractions inside the photonic crystals. However, the transmission information is gathered in all possible diffraction including scattering. The reflection offers information on selected diffraction phenomena determined by the geometry of the scattering, which is suitable for our purposes. The angular reflection spectra of p- and s-polarized light along L-U (U-K) direction are shown in Figs. 3(a) and 3(b), respectively, where the spectra are determined at increasing incident angles of 1° . The reflection peaks can be seen in these spectra throughout the range of incident angles, thus permitting an adequate evaluation of the polarization dependence. In addition, Figs. 3(c) and 3(d) provide the comparison between p-polarization, s-polarization, and un-polarization reflection spectra at two incident angles of $\theta = 0^\circ$ and 10° , respectively.

At the normal incident angle ($\theta = 0^\circ$), the reflection spectra have three peaks (P_1 - P_3), the strongest peak is located at 494 nm, and two weaker peaks are located at 478 and 460 nm. The strongest peak is very sharp with bandwidth about 11 nm ($\Delta\lambda/\lambda_0 = 2.2\%$). The reflection peaks and their bandwidths of p- and s-polarized light are similar to that of unpolarized light. It is reasonable that the optical properties at the small incident angle are nearly isotropic, and the effect of polarization dependence is manifested at the large incident angle.

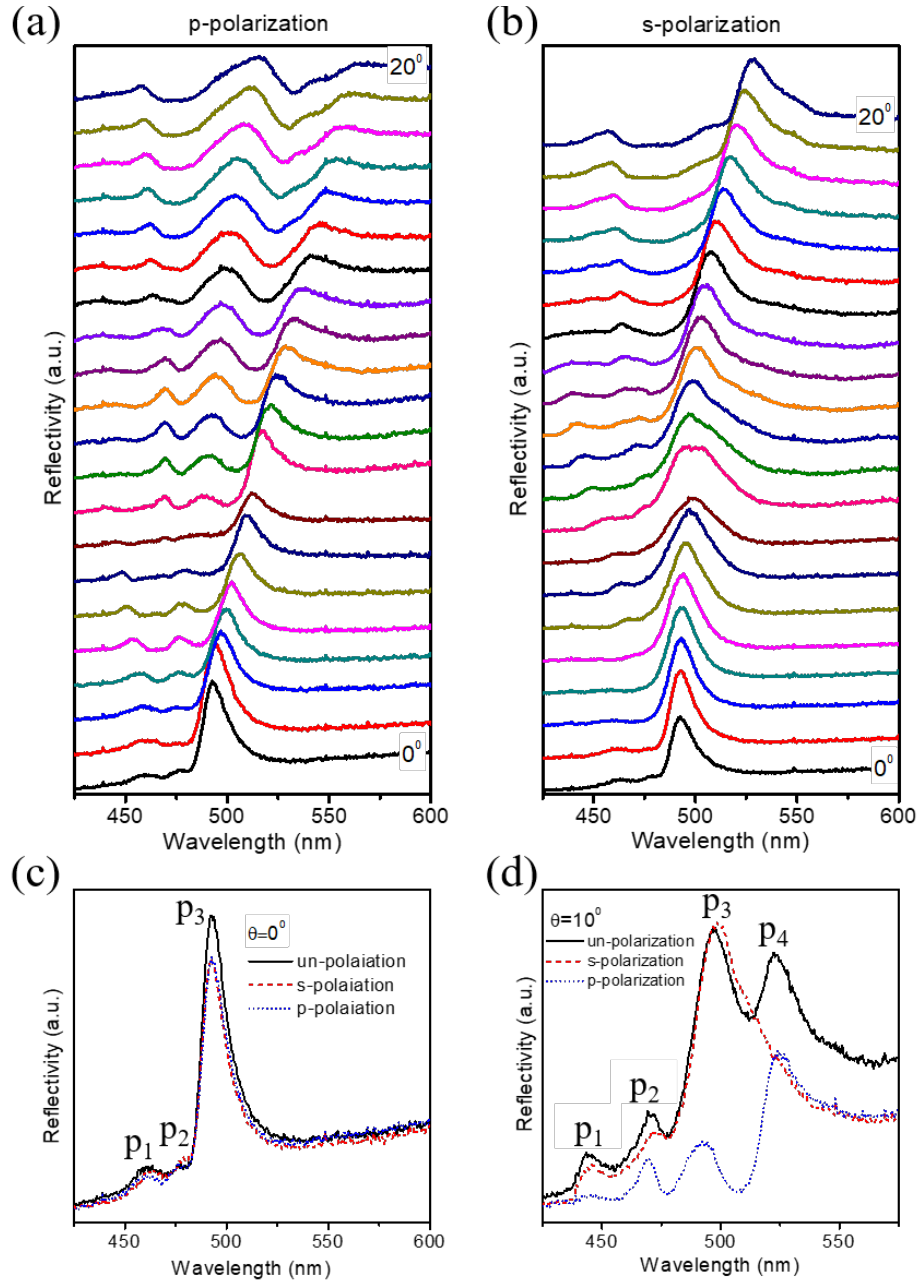


Fig. 3. Reflection spectra along L-U (U-K) direction of the opal PhC of silica with sphere diameter $D = 424\text{nm}$. (a) and (b) correspond to p-polarization and s-polarization, respectively. (c) and (d) reflection spectra at $\theta = 0^\circ$ and 10° with dashed (red), dotted (blue), and solid (black) lines corresponding to s-polarization, p-polarization, and un-polarization, respectively.

As the incident angles $\theta = 10^\circ$, the quite different reflection spectroscopy between two orthogonal s- and p-polarized lights is observed. The s-polarization has three peaks (447 nm; 475 nm; 501 nm), while the p-polarization has four peaks (446 nm; 470 nm; 492 nm; 523 nm) as denoted P₁-P₄ in Fig. 3(d). The peak positions of both s- and p-polarization in the shorter wavelength region (P₁ and P₂) are slightly shifted. However, the difference of other peaks is pronounced in the longer wavelength region (P₃ and P₄). As observed in Fig. 3(d), the reflection peaks of un-polarization are combination of both s- and p-polarization. The s-polarization has a bandwidth larger than p-polarization, and reflectivity of s-polarization is stronger than that of p-polarization. It indicates that the polarization dependence on high-order reflection spectra is more obvious at large incident angle.

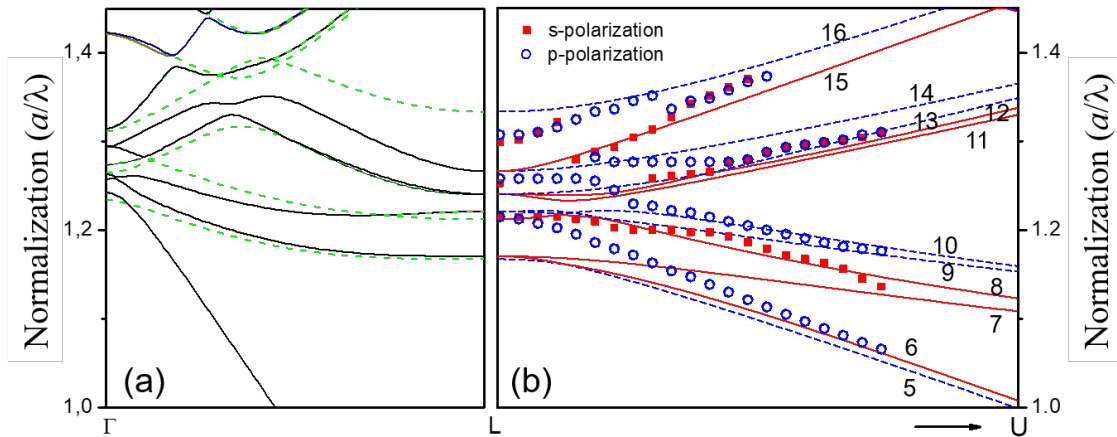


Fig. 4. Calculated band structure (lines) of opal PhC based on close packing fcc lattice along Γ -L (a) and L-U (b). Solid squares and empty circles correspond to measured s- and p-polarization, respectively, solid and dashed lines indicate calculated s- and p-polarization.

Detailed inspection of the dispersion of reflection peaks for two orthogonal light polarizations is compared with photonic band structure. We performed the simulated calculations using the RSoft to the fcc structure with refractive index $n = 1.46$ and sphere diameter $D = 424$ nm. Fig. 4(a) shows the band structure along Γ -L direction, where the solid line (black) and dashed line (green) correspond to coupled and uncoupled bands that is interpretative in Ref. 17. Fig. 4(b) shows the comparison of experimental peaks (square and circle) and band structure calculation (lines) along L-U direction. The squares (red) and circles (blue) correspond to s- and p-polarization of experimental reflection peaks, respectively, and solid (red) and dashed (blue) lines correspond to s- and p-polarization of photonic calculation [17]. The experimental results coincide fairly well with calculated photonic bands, and slight discrepancies can be explained by the imperfect structure of artificial opal PhCs. In the high energy region, the intermixture of many flat bands is involved to affect the optical phenomena that are more complex. In addition, the optical reflection on the

artificial opal has come in principle from considering the energy bands simultaneously with both of inside the Brillouin zone and its surface. The coupling efficiencies of the eigenmodes are not easy to visualize. It is also depending on the polarization of the incident light.

The reason causing the polarization dependence on high-order reflection spectra relates to the symmetry of opal eigenmodes in the photonic band with different behaviors [17], which will determine a different optical reflection due to two orthogonally polarized lights. With the combination of experimental result and photonic bands, the experimental results agree with the prediction based on group theory that show the calculated pairs of bands (7^{th} and 8^{th}) and (11^{th} and 12^{th}) coupled to s-polarized light, and the other pairs (9^{th} and 10^{th}) and (13^{th} and 14^{th}) coupled to p-polarized light [17]. However, observation in the pairs of bands (5^{th} and 6^{th}) and (15^{th} and 16^{th}) is quite different. We only see the optical reflection of p-polarization, whereas the pair of bands 5^{th} and 6^{th} corresponds with p- and s-polarization, respectively. In addition, the band 15^{th} corresponds with s-polarization, and the band 16^{th} corresponds with p-polarization, but the optical reflection of both s- and p-polarization is appearing. The optical reflection is an experimental evidence, which demonstrates the polarization dependence effects of interaction between polarized light and artificial opal PhCs. Due to symmetry properties of the structured lattice, the full understanding of physics origin of the complex interaction between polarized light and PhCs is worth further investigations.

IV. CONCLUSIONS

We have measured and analyzed polarization- and angle-resolved reflection from an artificial opal PhC. The results show interesting polarization dependence on high-order reflection. Observation of difference in optical reflection peaks at the same incident angles demonstrates the polarization dependence effect when light interacts with opal PhC. The experimental results fairly agree with calculated photonic bands, which is also confirmed by previous analysis results based on group theory.

ACKNOWLEDGEMENT

We acknowledge Prof. Chia Chen Hsu from National Chung Cheng University, Taiwan for his support in simulation. This research is funded by Vietnam National Foundation for Science and Technology Development (NAFOSTED) under Grant Number 103.02-2017.67.

REFERENCES

- [1] C. López, *Adv. Mater.* **15** (2003) 1679-1704.
- [2] K. Sakoda, *Optical Properties of Photonic Crystals*, Springer, New York, 2004.
- [3] J. D. Joannopoulos, S. G. Johnson, J. N. Winn, and R. D. Meade, *Photonic Crystals Molding the Flow of Light*, Princeton University Press, Princeton, 2008.
- [4] S. Furumi, H. Fudouzi, and T. Sawada, *Laser & Photon. Rev.* **4** (2010) 205-220.
- [5] R. Rengarajan, D. Mittleman, C. Rich, and V. Colvin, *Phys. Rev. B* **71** (2005) 016615.
- [6] L. A. Dorado and R. A. Depine, *Phys. Rev. B* **79** (2009) 045124.
- [7] V. N. Bogomolov, S. V. Gaponenko, I. N. Germanenko, A. M. Kapitonov, and E. P. Petrov, N. V. Gaponenko, A. V. Prokofiev, A. N. Ponyavina and N. I. Silvanovich, and S. M. Samoilovich, *Phys. Rev. E* **55** (1997) 7916.
- [8] S. G. Romanov, T. Maka, C. M. Sotomayor Torres, M. Müller, R. Zentel, D. Cassagne, J. Manzanares- Martinez and C. Jouanin, *Phys. Rev. E* **63** (2001) 056603.
- [9] L. D. Tuyen, C. Y. Wu, T. K. Anh, L. Q. Minh, H. C. Kan and C. C. Hsu, *J. Exp. Nanosci.* **7** (2012) 198-204.

- [10] A. Avoine, P. N. Hong, H. Frederich, J. M. Frigerio, L. Coolen, C. Schwob, P. T. Nga, B. Gallas and A. Maitre, *Phys. Rev. B* **86** (2012) 165432.
- [11] L. A. Dorado, R. A. Depine and H. Míguez, *Phys. Rev. B* **75** (2007) 241101(R).
- [12] J. F. Galisteo-López, F. López-Tejiera, S. Rubio, C. López, J. Sánchez-Dehesa, *Appl. Phys. Lett.* **82** (2003) 4068-4070.
- [13] A. V. Baryshev, A. B. Khanikaev, H. Uchida, M. Inoue and M. F. Limonov, *Phys. Rev. B* **73** (2006) 033103.
- [14] A. V. Baryshev, A. B. Khanikaev, R. Fujikawa, H. Uchida, and M. Inoue, *Phys. Rev. B* **76** (2007) 014305.
- [15] S. G. Romanov, *Phys. Solid State* **52** (2010) 844.
- [16] Priya and R. V. Nair, *Phys. Rev. A* **93** (2016) 063850.
- [17] F. López-Tejiera, T. Ochiai, K. Sakoda, J. Sánchez-Dehesa, *Phys. Rev. B* **65** (2002) 115110.
- [18] L. D. Tuyen, D. D. Bich, D. T. X. Thao, L. Q. Minh, and C. C. Hsu, *J. Sci. Tech. (Vietnam)* **54** (2016) 143-150
- [19] W. Stöber, A. Fink, and E. Bohn, *J. Colloid Interface Sci.* **26** (1968) 62-69.
- [20] G. Lozano, L. A. Dorado, D. Schinca, R. A. Depine and H. Míguez, *Langmuir* **25** (2009) 12860-12864.